

Anomalies and open issues of the MICROSCOPE Space Test of the Weak Equivalence Principle

Anna M. Nobili¹ and Alberto Anselmi²

¹*Dept. of Physics “E. Fermi”, University of Pisa, Largo B. Pontecorvo 3, 56127 Pisa, Italy*

²*Thales Alenia Space Italia, Strada Antica di Collegno 253, 10146 Torino, Italy (ret.)*

(Dated: May 4, 2023)

MICROSCOPE’s final results report no violation of the Weak Equivalence Principle (Universality of Free Fall) for Pt and Ti test masses quantified by an Eötvös parameter $\eta \simeq 10^{-15}$, an improvement by about two orders of magnitude over the best ground tests. The measurement is limited by random noise with $1/\sqrt{\nu}$ frequency dependence attributed to thermal noise from internal damping occurring in the grounding wires. From information available and the physics of internal damping we calculate the differential acceleration noise spectral density at the signal frequency, and show it varies widely between experiment sessions. Such large variations are inexplicable if translated into physical quantities such as the quality factor. While calibrations interspersed with measurement sessions may cause some such changes, they cannot explain jumps between consecutive sessions without recalibration. A potential explanation is conjectured related to a fluctuating zero depending on measurement initialization errors. The experiment was severely affected by “glitches” –anomalous acceleration spikes related to radiation from the Earth– injecting significant power at the signal frequency and its harmonics. The procedure used to deal with the glitches depends on introducing artificial data and leaves spurious effects potentially mimicking a violation signal or canceling a real one. An alternative procedure, relying only on real measured data, is proposed, already used in ground tests of the Weak Equivalence Principle by the *Eöt-Wash* group. Future experiments aiming to exploit the full potential of space must resolve these issues, rely solely on measured data, and, more generally, readdress the experiment design.

I. INTRODUCTION

MICROSCOPE is the first experiment on the Weak Equivalence Principle (WEP) performed in low Earth orbit. A potential violation of the WEP is quantified by the Eötvös ratio η , the fractional differential acceleration between two test masses of different composition as they fall in the gravitational field of a source body, the Earth in this case.

The instrument complement included two sensor units (SU), one with test masses (TM) of different composition for the WEP test (SUEP), the other with equal composition TM’s for control (SUREF). Each SU includes two test masses configured as coaxial hollow cylinders, the common axis being the sensitive axis. Each TM forms part of an independent accelerometer. A set of electrodes is used for both measuring the position of the TM and applying the voltages that maintain it “motionless” with respect to its cage. A thin gold wire provides electric grounding and polarization of the electrostatically levitated mass. TM motion is detected by capacitive sensing (displacements induce capacitance variations). In orbit, the axis of symmetry of the SU’s is in the orbit plane and a putative violation signal is an Earth pointing vector whose size oscillates at the orbit frequency of 1.6818×10^{-4} Hz plus or minus the satellite spin rate. In the valid experiment sessions, spin rates opposite the orbit motion were used, resulting in signal frequencies of $\nu_{EPV2} = 0.92499 \times 10^{-3}$ Hz and $\nu_{EPV3} = 3.11133 \times 10^{-3}$ Hz, the synodic frequencies relative to the Earth in V2 and V3 spin mode respectively.

The measurements were taken in sessions of 120 or

bits (8.26 days) or less, the upper limit being driven by periodic correction of clock drift. The experiment was affected by anomalous acceleration peaks (named “glitches”) occurring simultaneously in the four test masses. The issue arose in past geodesy missions and was solved in GOCE, mostly thanks to a stiffer solution for the multi-layer insulation. In MICROSCOPE glitches are found to produce large accelerations at the same frequency as the signal and its harmonics. In order to cope with glitches large portions of data were removed and replaced with artificial data.

Early results published in 2017 [1] were based, for the SUEP sensor, on the analysis of one measurement session (#218) lasting 8.26 days and reported a fractional difference of $\simeq 10^{-14}$ in the accelerations of Pt and Ti test bodies. A complete analysis of 94 days in 19 sessions reports no violation at the level of $\eta \simeq 10^{-15}$ [2, 3].

Establishing the nature and source of the noise limiting the measurement is crucial for any experiment and a prerequisite for future improvements. The early report [1] showed plots of the square root of the power spectral density (PSD) of the differential acceleration measured in two sessions, and the comment explicitly pointed out, in the frequency region of interest, a $1/\sqrt{\nu}$ trend attributed to random thermal noise from internal damping occurring in the gold wires. Two years later [4], an improved analysis of the same two sessions was interpreted in the same way. The final report [2] does not mention the limiting noise and no longer shows any PSD plot. In the batch of companion papers [3] only a couple of plots are provided [5], which appear to confirm the $1/\sqrt{\nu}$ trend. In one case [6] a potential minor contribution from elec-

trostatic patch noise is conjectured, with unknown frequency dependence. In general [3], wire damping is mentioned as the most likely cause but the authors seem to refrain from drawing any firm conclusions as to the nature of the noise. Lacking any contrary information, we assume the wire damping hypothesis in our analysis.

Systematic effects that were a matter of concern [7] turned out to be dominated by temperature variations; after calibration and a posteriori correction of all sessions, residual systematic errors were much smaller than random errors (SUEP) or close to them (SUREF) [5, 8].

The stiffness of the gold wires, whose damping gives rise to the dominant thermal noise, exceeds expectations based on ground tests by two orders of magnitude, in addition to showing unexplained features (Sec. II).

We first focus on the thermal noise and the physical parameters it depends upon: the stiffness and the quality factor of the wires. They are properties of the physical plant that must remain constant unless specific actions are undertaken which alter the instrument setup. Alterations may occur during calibrations, since they may offset the TM and affect the stiffness (Sec. II). However, an anomalous behavior of thermal noise occurs also in some sequential sessions not affected by calibrations, and even within the same session. We conjecture an explanation in terms of initialization errors (Sec. III).

Glitches are very numerous, between 14000 and 40000 in 120 orbits. They produce large effects at the frequency of the signal and its harmonics. In the procedure used to deal with glitches, many data points are removed and replaced with artificially reconstructed data. Such a procedure introduces new potential sources of error and is not mandatory. The WEP ground tests by the *Eöt-Wash* group [9] provide a successful example of data analysis in the presence of missing data carried out without introducing artificial data, exploiting the fact that the frequency and phase of the target signal are known. We suggest that such an analysis is the most appropriate and would definitively settle the experiment result (Sec. IV).

Conclusions are drawn in (Sec. V).

II. THERMAL NOISE FROM INTERNAL DAMPING WITH A HUNDREDFOLD HIGHER STIFFNESS

Once systematics have been taken care of –and if read-out noise is not an issue– the measurement is ultimately limited by random thermal noise. It sets the length of the integration time required for the signal to emerge. A thermal noise 10 times larger requires an integration time 100 times longer to detect the same signal [10].

In both sensors each TM constitutes an independent accelerometer. Unlike common mode effects, random noise is not reduced by taking the difference of the individual accelerations. Assuming that they are uncorrelated, the differential acceleration noise is obtained by adding them in quadrature.

In the case of internal damping, each test cylinder of

mass m is subjected to a thermal acceleration with a PSD whose square root is [11]:

$$S_{a_{th}}^{1/2}(\nu_{EP}) = \sqrt{4k_B T \cdot \frac{k}{m^2 Q} \cdot \frac{1}{\sqrt{2\pi\nu_{EP}}}} \quad (1)$$

with $k_B T$ (k_B the Boltzmann constant) the random disordered energy of thermal equilibrium at temperature T , k the stiffness and Q the quality factor of the wire, ν_{EP} the frequency of the target WEP violation signal.

WEP tests with rotating torsion balances operate close to the thermal noise limit due to dissipation in the suspension wire with quality factor $Q \simeq 6000$ [12]. In [13] various sources of thermal noise have been investigated for the GG proposed space test of the WEP, finding that gas damping (frequency independent) would contribute more than internal damping because the frequency of the signal is upconverted from the orbital frequency to the much higher spin frequency (1 Hz) in order to exploit the $1/\sqrt{\nu}$ dependence of internal damping noise [14].

Along the symmetry axis of MICROSCOPE test cylinders (the only one sensitive to WEP violation) displacements of the TM from the “zero” position are measured with the “area variation” principle rather than the “gap variation” principle used for the other two linear axes [15]. In the former case there should be no electrostatic stiffness, except for small boundary effects depending on the gap and larger for larger gaps. Instead, with “gap variation” the “zero” is a point of unstable equilibrium, the (negative) electrostatic stiffness exceeding the (positive) stiffness of the wire by far. A stiffness of $5 \times 10^{-5} \text{ Nm}^{-1}$ was measured for the “area variation” CAESAR accelerometer [15].

For each TM the total stiffness was measured in orbit by applying a large displacement signal and measuring the acceleration in response to it [16]. The acceleration over displacement ratio is k_{tot}/m and yields the total stiffness $k_{tot} > 0$, showing that the system behaves like a harmonic oscillator with natural frequency of oscillation $\omega_o = \sqrt{k_{tot}/m}$ forced at $\omega < \omega_o$. The stiffness measured is attributed entirely to the wire because it is found unaffected by the electric voltages [4]. Alas, it is two orders of magnitude bigger than in ground measurements [17].

An *ad-hoc* electrostatic torsion pendulum measured the stiffness of a wire by applying a force perpendicular to it, the theoretical prediction being $k_{\perp} = 3\pi E r^4 / \ell^3$ for a beam of radius r and length ℓ with $E = 7.85 \times 10^{10} \text{ Nm}^{-2}$ the elastic Young modulus of gold. The agreement was good and on that basis the expectation for the similar wire of the space experiment (3.5 μm radius, 2.5 cm length) was $k_{\perp} = 7 \times 10^{-6} \text{ Nm}^{-1}$, while the measured value is $\simeq 10^{-3} \text{ Nm}^{-1}$. Furthermore, although the four wires are all made of gold and all have the same geometry, their measured stiffnesses differ up to 7 times.

If the wire is attached parallel to the cylinder’s X axis –as we guess– only the radial stiffness (in any direction of the plane perpendicular to it) obeys the k_{\perp} formula, contributing a positive stiffness which is negligible if compared to the much larger electrostatic negative stiffness,

as it is confirmed by the measurements along the Y, Z axes [16]. Instead, for the sensitive X axis what matters is the stiffness under the effect of a force along the wire. For a beam with section πr^2 the theoretical stiffness under the effect of a longitudinal force is $k_{\parallel} = \pi r^2 E / \ell$, which in this case would be a huge factor 1.7×10^7 bigger than the expected k_{\perp} . This is not the case, hinting that the wire is, to some extent, slack.

It is argued [4] that the very large measured values may be due to a contribution from the stiffness along the axis of the wire, which comes into play if the wire is pushed or pulled along its axis. However, there is no indication as to how large this contribution would be and why it can vary so much. In [17] a sketch shows the wire under test as if it were slack, but the effect is not discussed. The fact is that the pendulum measures k_{\perp} , while what is needed is k_{\parallel} . Its dependence on the wire being more or less slack/taut is likely to make it vary between sessions if a calibration occurs in between, because in the calibration the quadratic acceleration term must be kept sufficiently small, which is achieved by offsetting the TM to a new “zero”, hence affecting k_{\parallel} . Since losses mostly occur at the two ends of the wire in correspondence of the glued points of attachment, they are unlikely to undergo substantial changes after launch, hence we expect the quality factor not to vary with calibrations.

Within the mission team, measurements [16] have been questioned by [18]. However, their model is incorrect: for a wire along the X axis it gives zero stiffness in the Y, Z directions, while it is $k_{\perp} = 3\pi E r^4 / \ell^3$.

A higher stiffness by $\lambda \simeq 100$ yields a higher thermal acceleration noise by $\sqrt{\lambda}$ (Eq. (1)), hence an integration time λ times longer to detect the same signal. The acceleration of the signal and systematics are unchanged, but produce λ times smaller displacements, the displacement being the physical quantity measured by each capacitance sensor. With the measured positive stiffness each electrostatically levitated TM is a harmonic oscillator with natural frequency of $\simeq 10^{-2}$ Hz.

III. ANALYSIS OF THERMAL NOISE AND OBSERVED ANOMALIES

For each sensor with TM's m_1, m_2 , stiffnesses k_1, k_2 , and the same Q for both masses (if not, the lower dominates), the square root of the PSD of the differential acceleration thermal noise is:

$$S_{\Delta a_{th}}^{1/2}(\nu) = f_{T_{kQ}} \cdot \frac{1}{\sqrt{2\pi\nu}} \quad (2)$$

with:

$$f_{T_{kQ}} = \sqrt{4k_B T \cdot \left(\frac{k_1}{m_1^2} + \frac{k_2}{m_2^2} \right) \cdot \frac{1}{Q}} \quad (3)$$

For a mechanical suspension the value of Q is known to be frequency dependent (higher at higher frequencies). However, the frequencies of interest in V2 or V3

spin mode are too close to expect any relevant difference in Q , and we therefore take $f_{T_{kQ}}$ as frequency independent. Hence, Eq.(2) represents, in a typical log-log plot (e.g. Fig. 2 of [1]), a straight line with negative 1/2 slope whose position along the vertical axis is set by the factor $f_{T_{kQ}}$ (in ms^{-2}).

For a given value of $f_{T_{kQ}}$ the measured noise is fitted by the same straight line. If the signal frequency increases, this noise decreases (as $1/\sqrt{\nu}$), but once the oscillator has been set up and launched, k 's and Q 's are fixed, and (except for a mild dependence on T) the value of $f_{T_{kQ}}$ is fixed and so is the straight line (2). However, after a calibration we cannot exclude a variation of the stiffness (Sec. II), hence of $f_{T_{kQ}}$ and of the spectral density of differential accelerations. To the contrary, in sequential sessions, or within the same session analyzed with equally valid methods, we expect no such variations.

In order to verify that the measured thermal noise does not change whenever it is expected not to, we need—for all measurement sessions—the spectral density of differential accelerations at the frequency of the signal. Since this quantity is not available in papers [2, 3] we derive it indirectly as follows.

At the frequency of the signal $S_{\Delta a_{th}}^{1/2}(\nu_{EP})$ given by (2) also obeys the equation [13]:

$$S_{\Delta a_{th}}^{1/2}(\nu_{EP}) = \sqrt{t_{int}} \cdot \delta \cdot g_{drive} \quad (4)$$

where $g_{drive} = 7.9 \text{ ms}^{-2}$ is the driving signal of WEP violation at the satellite orbit, t_{int} is the session duration and $\delta \cdot g_{drive}$ is a “nominal” violation signal with signal to noise ratio $\text{SNR}=1$ that would not be detected because of thermal fluctuations (σ), which decrease with the session duration as more data are available. For a given δ , the lower σ , the lower the integration time for a violation signal to emerge and be detected.

Tables 6, 7 in [5] give δ (and its σ) for all sessions based on two different methods of data analysis, named M and A (discussed below). In all sessions, except for SUREF sessions #294 and #380, the value of δ is smaller than 2σ [5]. With δ and the duration of the session [19], Eq. (4) gives $S_{\Delta a_{th}}^{1/2}(\nu_{EP})$; this value, using (2) at $\nu = \nu_{EP}$, yields $f_{T_{kQ}}$, from which—given the equilibrium temperature [5], the masses and the measured stiffnesses—the quality factor Q is inferred. An extensive series of ground measurements is available for comparison and validation [17]. Since k_1, k_2 may vary because of calibrations we compute also k/Q assuming the same unknown k for both TM's. These quantities are listed in Table I for SUEP and in Table II for SUREF, along with the percentage G of artificial data that have been introduced in each session after the elimination of glitches.

Tables I and II show that, contrary to expectations, large jumps in $S_{\Delta a_{th}}^{1/2}(\nu_{EP})$, Q and k/Q occur between sequential sessions (sessions are numbered by even numbers) in three cases for SUEP and in three cases for SUREF.

TABLE I. SUEP sensor. Session number in V2/V3 spin mode; session δ and percentage of glitches G from Tables 6,7 and 4,5 of [5]; calculated values of $S_{\Delta_{ath}}^{1/2}(\nu_{EP})$, Q , k/Q . \downarrow indicates a jump between sequential sessions; * an M vs A discrepancy.

Session	δ 10^{-15}		$S_{\Delta_{ath}}^{1/2}(\nu_{EP})$ $10^{-11} \text{ms}^{-2}/\sqrt{\text{Hz}}$		Q		k/Q 10^{-3}N/m		G %
	M	A	M	A	M	A	M	A	
\downarrow 210 (V3)	-30.1	-29.2	13	13	0.75	0.79	1.2	1.1	18
212 (V3)	10.4	9.5	4.9	4.5	5.2	6.3	0.17	0.15	17
*218 (V3)	3.6	6.7	2.4	4.5	22	6.3	0.042	0.14	15
234 (V3)	5.6	5.9	3.3	3.4	12	11	0.078	0.086	18
\downarrow 236 (V3)	2.7	2.6	1.8	1.7	39	42	0.024	0.022	21
238 (V3)	6.1	5.8	4.1	3.9	7.6	8.4	0.12	0.11	24
252 (V3)	-14.7	-14.9	9.2	9.3	1.5	1.4	0.62	0.64	26
\downarrow 254 (V3)	-14.2	-14.1	9.5	9.4	1.4	1.4	0.65	0.64	27
256 (V3)	-4.7	-5.3	3.1	3.5	13	10	0.071	0.091	28
326-1 (V3)	-10.1	-16.3	4.8	7.7	5.5	2.1	0.16	0.43	12
326-2 (V3)	-11.1	-10.4	3.9	3.7	8.1	9.2	0.11	0.099	7
358 (V3)	15.4	15.8	9.0	9.2	1.6	1.5	0.59	0.62	14
402 (V2)	27.3	28.4	7.1	7.3	8.5	7.9	0.11	0.12	35
*404 (V3)	6.3	4.7	4.2	3.1	7.1	13	0.13	0.071	23
406 (V3)	6.0	5.9	1.6	1.6	47	49	0.019	0.019	23
*438 (V2)	-12.5	-23.4	4.3	8.1	23	6.5	0.040	0.14	21
*442 (V2)	-10.7	-1.5	4.1	0.58	25	1273	0.037	0.00072	21
*748 (V2)	-17.5	-23.4	5.2	7.0	15	8.7	0.059	0.11	25
750 (V3)	66.6	66.9	11	12	0.97	0.95	0.94	0.97	19

Values of $Q < 1$ and close to critical damping observed in two SUEP sessions are unrealistic.

Two methods of analysis, M -ECM (M) and ADAM (A), have been employed to estimate the experiment parameters, including δ and σ . Both methods use artificially reconstructed data to account for the missing data resulting from the elimination of glitches.

Method M estimates in the time domain the missing data and then computes the least-squares estimate of the regression parameters, maximizing the likelihood conditional on the observed data. An estimation of the PSD is also produced in the process. Method A performs the parameter estimation in the frequency domain. As such it requires an uninterrupted, regularly spaced time series, which is obtained by filling the gaps left by the removal of glitches with the artificial data estimated by M .

The two methods are stated to be equivalent, leading to the same results, but in a few cases the δ 's calculated by M and A differ considerably (by a factor $\simeq 2$ in sessions #218, #438 and by a factor 7 in #442), implying that the same data stream leads to a different PSD according to one or the other method. Replicating the analysis by two (partially) independent methods is meant to enhance the confidence in the results, but the confidence is undermined if the methods give different results and the difference is not explained.

SUEP session #442 is an instructive extreme case. As reported in [5], Table 7, it has: $(\delta \pm \sigma)_M = (-10.7 \pm 19.0) \times 10^{-15}$, $(\delta \pm \sigma)_A = (-1.5 \pm 19.1) \times 10^{-15}$. That is, the noise is essentially the same but the values of δ differ by a factor 7; δ representing a “nominal” violation with SNR=1. How is it possible that, for the same measurement session, in the same experimental conditions, the same data with the same level of noise can lead to almost one order of magnitude difference in the evaluation of δ ?

The difference is particularly evident when the results

are interpreted in terms of the physics of the dominant thermal noise from internal damping (widely different Q 's, up to an embarrassing level in session #442).

SUREF session #778-1 is the only one, among all 32 measurement sessions (19 SUEP + 13 SUREF), not affected by glitches, hence it has no artificial data. In this case [5], Table 6, reports $(\delta \pm \sigma)_M = (-8.1 \pm 4.5) \times 10^{-15}$, $(\delta \pm \sigma)_A = (-8.1 \pm 4.7) \times 10^{-15}$. That is, the results are exactly the same for δ and only slightly different for σ , as one expects if the same data set is analyzed with two equally valid methods.

Sessions #442 and #778-1 show that the M and A methods are in agreement when applied to a time series of real measured data (no missing points and no reconstructed data), but give different results (in particular different δ 's) in the presence of artificial reconstructed data. Since the artificial data in A are those estimated by M , it is the way the two methods manipulate them that makes the difference. In any case, no matter how artificial data are generated and/or manipulated, they should not introduce any physical information, i.e. their effect on the δ estimated in each session ought to be null; otherwise, the more artificial data are used in a session, the more “artificial” will be the value of δ obtained for that session.

It is not clear whether the artificial data are included in the calculation of the σ 's. If they are, all σ 's are underestimated (the more dummy data, the lower the noise), and this has an impact on the reported global result (weighted by σ^{-2}) whose noise would be underestimated too.

TABLE II. Same as Table I for SUREF sensor. A \bullet has been added to indicate sessions with Q values much larger than the largest value of 118 measured in ground tests [17].

Session	δ 10^{-15}		$S_{\Delta_{ath}}^{1/2}(\nu_{EP})$ $10^{-11} \text{ms}^{-2}/\sqrt{\text{Hz}}$		Q		k/Q 10^{-3}N/m		G %
	M	A	M	A	M	A	M	A	
\downarrow *120-1 (V2)	-3.1	-4.2	0.89	1.2	268	146	0.042	0.077	4
120-2 (V2)	-16.8	-15.1	8.2	7.4	3.1	3.9	0.36	0.29	15
\downarrow 174 (V2)	7.8	8.0	4.4	4.5	11	10	0.10	0.11	25
\bullet 176 (V2)	1.7	1.8	0.82	0.86	317	283	0.0036	0.0040	40
294 (V3)	-8.0	-7.7	4.2	4.1	3.5	3.7	0.33	0.30	17
376-1 (V2)	-3.4	-4.1	1.2	1.5	135	93	0.0083	0.012	14
376-2 (V2)	-5.7	-6.4	1.8	2.1	62	49	0.018	0.023	11
380-1 (V3)	7.6	7.4	3.1	3.1	6.4	6.7	0.18	0.17	7
380-2 (V3)	9.3	8.9	3.3	3.2	5.7	6.3	0.20	0.18	5
452 (V2)	-4.3	-4.8	1.5	1.7	101	81	0.011	0.014	20
454 (V2)	-3.1	-3.7	1.4	1.7	111	78	0.010	0.014	22
\downarrow 778-1 (V2)	-8.1	-8.1	3.0	3.0	23	23	0.049	0.049	0
* \bullet 778-2 (V2)	-2.3	-3.2	0.59	0.83	599	309	0.0019	0.0036	6

In SUEP session #218, the values of δ differ by a factor of about 2 depending on the type of analysis. This session (120 orbits) was the basis of the early results [1], and was further elaborated two years later [4], ending up with a different value of the spectral density at the signal frequency. Even discarding the earlier results because systematics had not yet been reduced and/or glitches had not yet been treated, it is apparent that even the latest analysis cannot be considered conclusive. Q values differing by a factor 3.5, for the same oscillator in the same conditions, are inexplicable.

The reference sensor SUREF behaves quite differently from SUEP. Thermal noise is about a factor $\sqrt{2}$ smaller than for SUEP (assuming the same Q), due to a factor 2 larger ($k_1/m_1^2 + k_2/m_2^2$) term, and residual systematic errors are comparable to the stochastic errors [5]. Moreover, 4 out of 9 sessions have been split because of sudden jumps in the mean value of the differential acceleration that required the two data segments to be treated as distinct experiments. Unlike glitches these jumps do not occur on all accelerometers, hence they cannot be attributed to the spacecraft but are likely to originate in the accelerometers themselves, and last much longer (tens of seconds). In SUEP only 1 session (#326) out of 18 has been split. In SUREF, in addition to the three cases mentioned above of anomalous jumps in $S_{\Delta a_{th}}^{1/2}(\nu_{EP})$, Q and k/Q in sequential sessions, we observe three sessions with large M vs A discrepancies (see Table II). However, the values of Q are typically larger than in SUEP and in three cases much larger than the largest value of 118 reported in ground measurements [17].

Early results [1] were based on session #176 (62 orbits). The spectral density $S_{\Delta a_{th}}^{1/2}(\nu_{EP})$ reported in [1] was confirmed in [4] and attributed to $1/\sqrt{\nu}$ thermal noise, yielding $\delta = 3.75 \times 10^{-15}$ and $Q = 65$, consistent with ground measurements. Instead, the final values of δ_M and δ_A are much smaller (Table II), and the corresponding Q 's of 317 and 283 are far too high to be realistic on the basis of ground tests. Note that session #176 has 40% of reconstructed data.

An explanation of the anomalies observed in sequential sessions may be conjectured as follows.

Accelerations are inferred (after calibration) from displacements measured with very high precision relative to a position assumed as a zero force point that the TM of each independent accelerometer is forced to maintain at all times. This capacitance zero is affected by inevitable uncertainties; it may change after calibration, and after initialization of a new session.

Within this design an elastic force much larger than expected was found to dominate the motion of each levitated TM. The zero of the elastic force and the capacitance zero that the TM is forced to, are unlikely to coincide, but the problem has not been investigated. With a large stiffness, and a dominant elastic force, the issue of an unstable zero is especially relevant because the elastic force is linear with the displacement from its physical zero to the capacitance zero (as in the case of the tidal force).

Aside from the gold wire, an unstable zero is an issue of its own in measuring the effects of extremely small forces. In WEP tests it is related to the problem of initial conditions (or release) errors that affect all experiments which are not intrinsically null experiments, including those with laser tracked satellites, celestial bodies and cold atoms [20–23]. Instead, in torsion-balance tests and the proposed GG space experiment the physical observable is a true null [24].

IV. GLITCHES, GAPS AND RECONSTRUCTED DATA

The experiment was plagued by anomalous short-duration (< 5 s) acceleration spikes originating in the spacecraft and occurring simultaneously in the four test masses.

Since 2001 five space missions carrying ONERA's ultra-sensitive accelerometers have been launched – CHAMP, GRACE, GOCE, GRACE Follow-On (GFO) and *MICROSCOPE* – with a total of seven satellites, and all but one have experienced such spikes (named “clanks” in CHAMP and GOCE, “twangs” in GRACE, “glitches” in *MICROSCOPE*). At the time of the design of GOCE, reports of such effects in CHAMP caused alarm, and countermeasures were adopted at design and test level, which were successful, and no spikes were seen. The succeeding missions discovered the problem anew.

Although as far as we know a comprehensive analysis across all the missions has not been carried out, there seems to be a consensus that the spikes are triggered by energy input from the Earth causing micro-vibration, e.g. release of stress energy in the spacecraft materials such as the multi-layer insulation (MLI) [25, 26]. Alternative hypotheses point to small electric discharges in the spacecraft surfaces, or changes in the solar array currents. The GOCE countermeasures program was based on the mechanical hypothesis, and in GFO a stiffer design of the nadir insulating foil has been adopted, thus, too, assuming a mechanical origin of the spikes.

Most important for the *MICROSCOPE* test of the WEP, the spacecraft is spinning, hence the occurrence of glitches is not random but it correlates with the synodic frequency of the spacecraft relative to the Earth (i.e. the frequency of WEP violation), and its harmonics.

In Ref. [27] it is concluded that glitches must be removed from the data because it is impossible to accurately model their effects. In the time series of every session glitches are identified as all outliers above 4.5σ from the moving average, some time is allowed before and after each outlier to account for transient effects, and all data points identified in this way are removed, up to 35% in SUEP and up to 40% in SUREF. By comparison, in the *Eöt-Wash* experiment the amount of data removed due to sporadic spikes in the ion pump current, or due to abrupt changes of the turntable axis from the local vertical, was 7% of the total [9].

For *MICROSCOPE*, unlike *Eöt-Wash*, the choice has been made to reconstruct the missing data.

An interesting comparison is reported in [27] between the FFT of the differential acceleration as obtained from the original measured data, and the FFT after glitches were removed and the missing data were reconstructed. This was done for SUREF session #380 lasting 120 orbits (of which two segments of 46 and 34 orbits each have been used in the final analysis) Fig. 1, copied from Fig. 10 in [27], shows the two plots, measured data in black, reconstructed data in red.

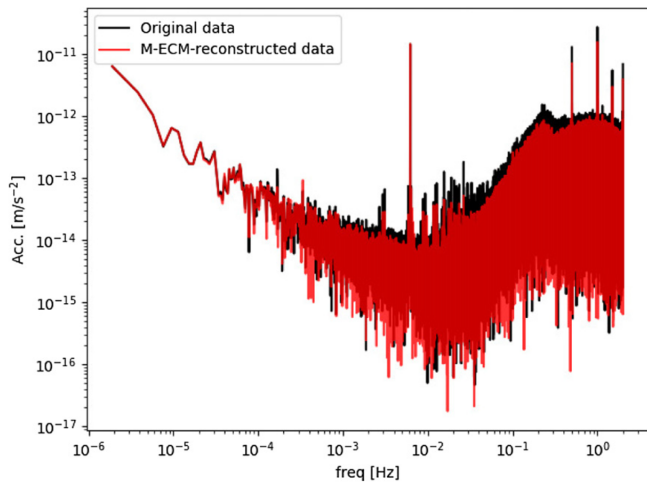


FIG. 1. Same as Fig.10 in [27], where the caption reads: “Spectra of SUREF’s x axis differential acceleration for session 380, before (black) and after (red) glitches masking and data reconstruction.” (x is the sensitive axis of the sensor)

This session is in V3 mode, hence the synodic frequency relative to the Earth is $\nu_{EPV3} = 3.1 \times 10^{-3}$ Hz, at which no WEP violation is expected. At this frequency the black curve in Fig.1 shows a differential acceleration line of 6 to $7 \times 10^{-14} \text{ m s}^{-2}$. Lines at $2\nu_{EPV3}$, $3\nu_{EPV3}$, $4\nu_{EPV3}$ and $5\nu_{EPV3}$ are visible too, indicating that glitches produce effects not only at the signal frequency but at its higher harmonics as well.

The largest effect occurs at $2\nu_{EPV3}$ and is dominated by the main component of the Earth tide; it must appear both in the original and in the reconstructed data, hence we guess that the black line is hidden behind the red line. The tidal effect at twice the signal frequency, being deterministic, is modelled to derive the offset between the TM’s, which is then used to quantify and subtract the tidal component at the same frequency and phase as the signal. Therefore the glitch effect at twice the signal frequency must be sufficiently smaller than the tidal effect at the same frequency. If the physical origin of the glitches is related to thermal energy from the Earth, one expects a non-negligible glitch component with half the synodic period, as the spacecraft goes from facing deep space to facing the warm planet.

After glitches have been removed and gaps have been filled with reconstructed data (46% of the total according to [27]), the red curve in Fig.1 shows a reduction of the lines previously ascribed to glitches. At twice the signal frequency the reduction cannot be quantified because of the dominant tidal effect.

More importantly, the pattern of lines related to glitches shows that the FFT based on the reconstructed data retains memory of the removed glitches. The reconstructed data, like the gaps, must necessarily follow the glitches, which have specific frequencies, hence the imprinting of glitches in the reconstructed data. Such a spurious effect at the signal frequency would mimic a

violation signal or cancel a real one.

To demonstrate the correctness of the procedure, a fake violation signal was injected in the data before preprocessing, and two reconstructed data sets were built from the original set (one without and one with the fake signal) from which two values of δ are recovered: if their difference yields the fake signal this is taken as evidence that the reconstructed data provide a reliable representation of the real measured data. However, the glitch spikes are so large that their removal is not affected by the fake signal; the resulting gaps follow the pattern of the frequencies at which glitches occur, and so do the data generated to fill them, as shown in Fig.1. Thus, the two reconstructed data sets are the same except for the fake signal, which is obviously recovered.

The use of a fake signal also shows a specific anomaly. In the only case without glitches, SUREF session #778-1, when a fake signal was added with $\delta_{fake} = 3.4 \times 10^{-14}$, it was recovered with the largest error of all other SUREF and SUEP sessions to which the same fake signal was added ([5], Table 8 and Sec.5.6), somehow suggesting that real data may in fact be more noisy than those containing artificial data. To make things even more confusing, when the fake signal added to the same session is 10 times weaker, it is recovered correctly.

Filling the gaps is mandatory as long as the analysis is performed in the frequency domain. However, a different approach is possible because the frequency and phase of a differential acceleration due to WEP violation in the field of a source body (the Earth in this case) are known; only its amplitude and sign are unknown.

At any given time, in the reference frame rotating with the MICROSCOPE spacecraft, the position of the Earth and the phase of the sensitive axis are known, and the offset of the TM’s can be derived from the tidal effect. Hence, in the time series of differential accelerations the violation signal is a sinusoid with the synodic period of the spacecraft relative to the Earth (at zero spin it would coincide with the orbital period) whose maximum size (unknown) occurs twice per synodic period when the sensitive axis of the sensor points towards or away from Earth (sign unknown). This demodulated phase lock-in signal can be fitted to the time series of the differential acceleration data –only the real measured data– in order to determine its amplitude and sign, which therefore would not be affected by whatever gaps.

In addition, lock-in detection makes it possible to separate spurious effects that have the same frequency of the signal, but not the same phase, as in the case of the glitch-induced effect (provided the spurious effect is not much bigger). Although both the glitch and the signal come from the Earth, it is very unlikely that the sensitive axes point exactly to the center of mass of the Earth when the glitch effect is maximum. Therefore, should a residual spurious effect remain after the elimination of glitches, it would not be confused with the signal.

A procedure of this kind has been successfully used in the *Eöt-Wash* ground tests of the WEP [9, 12]. The same

procedure, applied to the MICROSCOPE data, would establish beyond question that the result of the experiment is not affected by the gaps and the artificial data generated to fill them.

V. CONCLUSIONS

A space test of the weak equivalence principle in the field of the Earth has enormous potential for a leap forward in precision, by building on a strong driving signal and better instrument isolation in space than in any ground laboratory, hence easier control of systematic effects from local disturbances. A satellite test of the WEP has been over 40 years in the making, a number of designs were proposed, one -MICROSCOPE- has made it to flight, and has reported two orders of magnitude improvement over the best laboratory experiments to date [2].

This work points at anomalies in the experiment and in the data analysis that need to be addressed for the experiment result to be consolidated, and to help designing a better space test of the future.

The MICROSCOPE experiment appears to be limited by thermal noise from damping in the grounding wires. Using the published information [3] we calculate the PSD for all sessions, and express it in terms of the dominant thermal noise and the physical quantities it

depends upon. Anomalous jumps are observed in sequential sessions (and even within the same session); the corresponding quality factors vary widely and are sometimes unrealistically high or low. We suggest an unstable zero may be the cause of such fluctuations, an issue that would require careful investigation even if the grounding wire were to be replaced by an active discharger.

The experiment was plagued by a large number of “glitches”, anomalous releases of energy, originating in the spacecraft, producing large differential accelerations at the signal frequency and its harmonics. We find evidence that the way they were treated (removed and replaced with artificial reconstructed data) leaves extant effects at the critical frequencies that could mimic a violation signal or cancel a real one. We suggest that an analysis as successfully employed in the *Eöt-Wash* laboratory tests, would be tolerant of the missing data without affecting the sensitivity of the experiment.

Any future WEP experiment in space must prove by its very design that it will not suffer from glitches (GOCE showed the way), and must avoid introducing artificial data potentially compromising the analysis. Over and above that, future experiments aiming to exploit the full potential of space must readdress the experiment design: null experiment, stable zero, minimal thermal noise by fast spin [7, 24].

-
- [1] P. Touboul *et al.*, MICROSCOPE Mission: First Results of a Space Test of the Equivalence Principle, *Phys. Rev. Lett.* 119, 231101 (2017).
 - [2] P. Touboul *et al.*, MICROSCOPE Mission: Final Results of the Test of the Equivalence Principle, *Phys. Rev. Lett.* 129, 121102 (2022).
 - [3] Special Issue of Classical and Quantum Gravity on MICROSCOPE, *Class. Quantum Grav.* 39, 20 (2022).
 - [4] P. Touboul *et al.*, Space test of the equivalence principle: first results of the MICROSCOPE mission, *Class. Quantum Grav.* 36, 225006 (2019).
 - [5] P. Touboul *et al.*, Result of the MICROSCOPE weak equivalence principle test, *Class. Quantum Grav.* 39, 204009 (2022).
 - [6] F. Liorzou *et al.*, MICROSCOPE instrument description and validation, *Class. Quantum Grav.* 39, 204002 (2022).
 - [7] A. M. Nobili and A. Anselmi, Testing the equivalence principle in space after the MICROSCOPE mission, *Phys. Rev. D* 98, 042002 (2018).
 - [8] M. Rodrigues *et al.*, MICROSCOPE: systematic errors, *Class. Quantum Grav.* 39, 204006 (2022). Note: The total residual systematic errors in Tables 13, 14 are incorrect. For the correct values see Tables 10, 11 in [5].
 - [9] S. Schlamminger, K.-Y. Choi, T. A. Wagner, J. H. Gundlach, and E. G. Adelberger, Test of the equivalence principle using a rotating torsion balance, *Phys. Rev. Lett.* 100, 041101(4p) (2008).
 - [10] A. M. Nobili *et al.*, ‘Galileo Galilei’ (GG): space test of the weak equivalence principle to 10^{-17} and laboratory demonstrations, *Class. Quantum Grav.* 29, 184011 (2012).
 - [11] P. R. Saulson, Thermal noise in mechanical experiments, *Phys. Rev. D* 42, 2437 (1990).
 - [12] T. D. Wagner, S. Schlamminger, J. H. Gundlach, and E. G. Adelberger, Torsion-balance tests of the weak equivalence principle, *Class. Quantum Grav.* 29, 184002 (2012).
 - [13] A. M. Nobili *et al.*, Integration time in space experiments to test the equivalence principle, *Phys. Rev. D* 89, 042005 (2014).
 - [14] R. Pegna, A. M. Nobili, M. Shao, S. G. Turyshev, G. Catastini, A. Anselmi, R. Spero, S. Doravari, G. L. Comandi, and A. De Michele, Abatement of Thermal Noise due to Internal Damping in 2D Oscillators with Rapidly Rotating Test Masses, *Phys. Rev. Lett.* 107, 200801 (2011).
 - [15] V. Josselin, P. Touboul, and R. Kielbasa, Capacitive detection scheme for space accelerometers applications, *Sensors and Actuators* 78, 92–98 (1999).
 - [16] R. Chhun *et al.*, Microscope instrument in-flight characterization, *Class. Quantum Grav.* 39, 204005 (2022).
 - [17] E. Willemonot, and P. Touboul, On-ground investigation of space accelerometers noise with an electrostatic torsion pendulum, *Rev. of Sci. Instrum.* 71, 302 (2000).
 - [18] J. Bergé, M. Pernot-Borràs, J.-P. Uzan, P. Brax, R. Chhun, G. Métris, M. Rodrigues, and P. Touboul, MICROSCOPE’s constraint on a short-range fifth force, *Class. Quantum Grav.* 39, 204010 (2022).
 - [19] M. Rodrigues *et al.*, MICROSCOPE mission scenario, ground segment and data processing, *Class. Quantum Grav.* 39, 204004 (2022).
 - [20] J. P. Blaser, Can the equivalence principle be tested with freely orbiting masses?, *Class. Quantum Grav.* 18, 2509

- (2001).
- [21] G. L. Comandi, A. M. Nobili, R. Toncelli, and M. L. Chiofalo, Tidal effects in space experiments to test the equivalence principle: implications on the experiment design, *Phys. Lett. A* 318, 251 (2003).
 - [22] A. M. Nobili, G. L. Comandi, D. Bramanti, Suresh Doravari, D. M. Lucchesi, and F. Maccarrone, Limitations to testing the equivalence principle with satellite laser ranging, *Gen. Relativ. Gravit.* 40, 1533 (2008).
 - [23] A. M. Nobili, Fundamental limitations to high-precision tests of the universality of free fall by dropping atoms, *Phys. Rev. A* 93, 023617 (2016).
 - [24] A.M. Nobili, and A. Anselmi, Relevance of the weak equivalence principle and experiments to test it: Lessons from the past and improvements expected in space, *Phys. Lett. A* 382, 2205 (2018).
 - [25] F. Landerer *et al.*, Extending the Global Mass Change Data Record: GRACE Follow-On Instrument and Science Data Performance, *Geophys. Res. Lett.* 47, e2020GL088306 (2020).
 - [26] N. Peterseim, Twangs – High Frequency Disturbing Signals in 10 Hz Acceleration Data of the GRACE Satellites. Dissertationen, Heft Nr. 735, Bayerische Akademie der Wissenschaften (2014).
 - [27] J. Bergé, Q. Baghi, A. Robert, M. Rodrigues, B. Foulon, E. Hardy, G. Métris, S. Pires, and P. Touboul, MICROSCOPE mission: statistics and impact of glitches on the test of the weak equivalence principle, *Class. Quantum Grav.* 39, 204008 (2022).
 - [28] Q. Baghi, G. Métris, J. Bergé, B. Christophe, P. Touboul, and M. Rodrigues, Gaussian regression and power spectral density estimation with missing data: The MICROSCOPE space mission as a case study, *Phys. Rev. D* 93, 122007 (2016).